

# To see the exotic $\Theta^+$ baryon from interference

Moskov Amarian<sup>a</sup>, Dmitri Diakonov<sup>b,c</sup>, and Maxim V. Polyakov<sup>b,c</sup>

<sup>a</sup> *Old Dominion University, Norfolk, Virginia 22901, USA*

<sup>b</sup> *Petersburg Nuclear Physics Institute, Gatchina, 188 300, St. Petersburg, Russia*

<sup>c</sup> *Institut für Theoretische Physik II, Ruhr-Universität Bochum, Bochum D-44780, Germany*

(Dated: December 12, 2006)

Since all couplings of the exotic  $\Theta^+$  baryon to normal hadrons seem to be small it is hard to reveal it in standard resonance searching. We suggest to look for the  $\Theta^+$  production in interference with a known resonance yielding the same final state but having a high production rate. The interference process is linear in the  $\Theta^+$  couplings whereas the non-interference process is quadratic. That gives an obvious gain if the couplings are small. Moreover, employing the peculiar oscillating nature of the interference processes one can reduce considerably the parasitic background and determine the  $\Theta^+$  resonance parameters.

PACS numbers: 12.38.-t, 12.39.-x, 12.39.Dc, 14.20-c

## I. INTRODUCTION

The original observation of a narrow exotic baryon resonance in two independent experiments by T. Nakano *et al.* [1] and A. Dolgolenko *et al.* [2], announced in the end of 2002 [3] were followed in 2003-04 by a dozen experiments confirming the resonance and about the same amount of non-sighting experiments. In 2005 the results of the two CLAS high-statistics  $\gamma d$  and  $\gamma p$  experiments were announced [5, 6, 7], which didn't see any statistically significant signal of the  $\Theta^+$  resonance and gave upper bounds for its production cross sections. Although those upper bounds didn't contradict the theoretical estimates [8, 9, 10], see also [11], many people in the community jumped to the conclusion that "pentaquarks do not exist". This conclusion is premature as in 2005-06 new results became available [12, 13, 14] partly based on new data, confirming seeing the  $\Theta^+$ .

In particular, A. Dolgolenko *et al.* [13] have doubled the statistics of their  $K^+n(\text{Xe}) \rightarrow K^0 p$  data as compared to the original DIANA experiment [2]. Previously, there were about 30 events attributed to the  $\Theta^+$  resonance, now there are about 60, as it should be if the signal is real. Also, more thorough analysis has been performed to understand better the kinematics of the reaction and the background processes. The resonance peak is seen already in the raw data but is strongly enhanced by a mild kinematical cut suppressing re-scattering. The authors estimate the statistical significance of the resonance as  $S/\sqrt{B} = 7.3\sigma$ . The mass is found to be  $m_\Theta = 1537 \pm 2 \text{ MeV}$  and the width  $\Gamma_\Theta = 0.36 \pm 0.11 \text{ MeV}$  (with possible systematic uncertainties). This is the only experiment where the direct estimate of the width is possible since the *formation* cross section integrated over the resonance range is proportional to the width [15]. The only other available formation experiment with the secondary kaon beam at BELLE sets an upper limit  $\Gamma_\Theta < 0.64 \text{ MeV}$  (at a 90% confidence level) [16] which is beyond the above value. We remark that the reanalysis of the old  $KN$  scattering data [17] shows that there is room for the exotic resonance with a width below 1 MeV.

The small width implies that the coupling  $g_{\Theta NK}$  is at least an order of magnitude less than  $g_{NN\pi} \approx 13$ . The small value of  $g_{\Theta NK}$  appears naturally in a relativistic field-theoretic approach to baryons, allowing for a consistent account for multi-quark components in baryons; in particular in Ref. [18, 19] an upper bound  $\Gamma_\Theta \approx 2 \text{ MeV}$  has been obtained without any parameter fixing. An even smaller width comes out from the parameter-free QCD sum rules analysis [20]. As to the  $\Theta^+$  coupling to the vector  $K^*$  meson, its 'electric' part corresponding to the  $\gamma_\mu$  vertex is anyway very small as it vanishes at zero momentum transfer in the  $SU(3)$ -symmetric limit, and its 'magnetic' part corresponding to  $\sigma_{\mu\nu}q_\nu$  is proportional to the  $\Theta N$  transition magnetic moment which is expected to be an order of magnitude less than the nucleon magnetic moments [21]. In fact, all  $\Theta^+$ -nucleon-meson couplings vanish in the imaginary non-relativistic limit when ordinary baryons are made of three quarks only with no admixture of  $Q\bar{Q}$  pairs. This was the base for the prediction of a narrow pentaquark in the first place [4].

If indeed all  $\Theta^+$ -nucleon-meson transition amplitudes are as small as are expected, it becomes a non-trivial task to reveal  $\Theta^+$  in *production* (as contrasted to formation) experiments. For example, in the recent study of the  $\gamma p \rightarrow K^0 \bar{K}^0 p$  reaction by CLAS collaboration no statistically significant resonance structure was observed despite record statistics, and only an upper limit of the  $\Theta^+$  production cross sections of  $\sim 0.7 \text{ nb}$  was obtained [7, 22]. However, a theoretical estimate performed prior to the experiment and based on the (Reggeized)  $K^*$  exchange with the small transition magnetic moment mentioned above, gave only  $\sim 0.2 \text{ nb}$  for that cross section [10]. [Recent phenomenological analysis of the  $K^*$  coupling to the antidecuplet [23] has confirmed its smallness.] It demonstrates how hard it is to make a definite conclusion about the  $\Theta^+$  existence from a production experiment employing a standard resonance-searching procedure.

In this paper, we suggest to search for the narrow  $\Theta^+$  resonance in a non-standard way, exploiting the interference of the small  $\Theta^+$  production amplitude with the large production amplitude of a known resonance, yielding the

same final state. Although the interference idea is very general, we apply it primarily to the CLAS experiment [7] whose impressive amount of data can be used to look for the  $\Theta^+$  resonance in interference with the large  $\phi$  photo-production, see Fig. 1. Since the final state in both cases is the same, the two amplitudes *must* interfere unless forbidden kinematically. A simple account for kinematics shows that the two amplitudes interfere within the photon lab energy range  $1.74 < E_\gamma < 2.15$  GeV which is inside the range studied by CLAS.

The  $\Theta^+$  production amplitude *squared* has been estimated in Ref. [10] with the tiny result for the cross section in the sub-nanobarn range – too small to be observable even with the large CLAS statistics. However, the interference cross section is *linear* in the  $\Theta^+$  coupling and hence can be substantially larger. In addition, the interference cross section has a peculiar oscillating nature which may help to establish the resonance mass and width without resolving the Breit–Wigner peak, which is impossible because it is so narrow.

## II. THE $\gamma p \rightarrow K^0 \bar{K}^0 p$ REACTION

### A. $K^0 \bar{K}^0$ versus $K_L K_S$

In the recent CLAS experiment [7] studying the above reaction,  $K_S$  (decaying into  $\pi^+ \pi^-$ ) and  $p$  have been detected. The second kaon was reconstructed from the missing mass of all detected particles. A large portion of events were due to the production of the  $\phi$  meson decaying into  $K_L K_S$ . These events have been rejected in the previous analysis [7], however they are exactly what are needed now: Fig. 1, right. Since  $\phi$  is a vector meson, the amplitude is antisymmetric under the interchange of  $K_L$  and  $K_S$ .

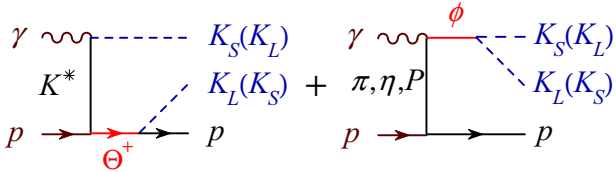


FIG. 1: Two  $\gamma p$  processes producing the  $K_L K_S p$  final state: via the  $\Theta^+$  resonance (left) and via the  $\phi$  resonance (right).

Since  $\Theta^+$  has strangeness +1 it necessarily decays into  $K^0$ , hence the upper line in Fig. 1, left, is  $\bar{K}^0$ . Using  $K^0 = (K_S + K_L)/\sqrt{2}$ ,  $\bar{K}^0 = (K_S - K_L)/\sqrt{2}$  (we neglect the one-per-mill effect of CP violation) one rewrites the  $(\bar{K}^0 K^0)$  production amplitude via  $\Theta^+$  as  $\frac{1}{2}(K_S K_S) - \frac{1}{2}(K_L K_L) + \frac{1}{2}(K_S K_L) - \frac{1}{2}(K_L K_S)$ . Only the last two terms interfere with the above amplitude of  $\phi$  production, and we see that they are also antisymmetric under the interchange of  $K_L$  and  $K_S$ . The two antisymmetric amplitudes can and do interfere; the resulting interference cross section is symmetric under  $K_L \leftrightarrow K_S$ .

### B. Kinematics

The  $2 \rightarrow 3$  reaction is characterized, at given values of masses of final particles, by 5 invariants, one of them being the invariant reaction energy  $\sqrt{s}$ . In this case  $s = m_N^2 + 2m_N E_\gamma$  where  $E_\gamma$  is the energy of the incoming photon in the proton rest (or lab) frame. The other two invariants can be chosen to be the invariant masses of  $K_L K_S$  (call it  $m_{12}$ ) and of  $K_S p$  (call it  $m_{23}$ ). The last two invariants can be chosen more or less arbitrarily. The phase volume of the reaction in the  $(m_{12}, m_{23})$  axes is shown, for various photon energies, in Fig. 2.

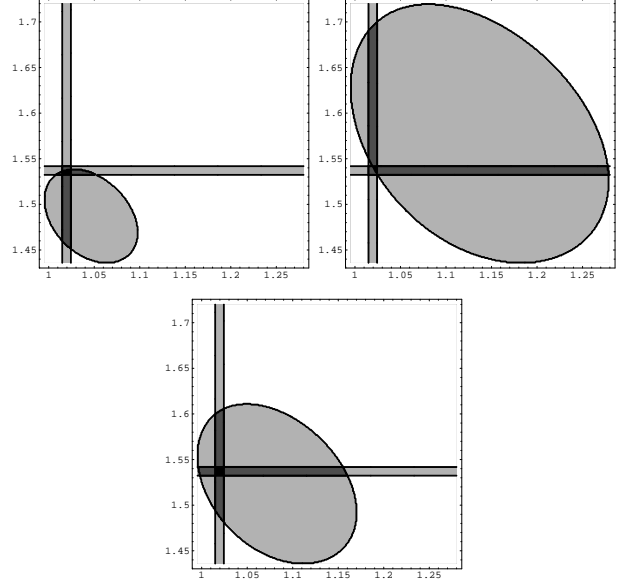


FIG. 2: Phase volumes (Dalitz plots) for the  $\gamma p \rightarrow K_L K_S p$  reaction at photon lab energies  $E_\gamma = 1.74, 2.15$  and  $1.90$  GeV. The  $K_L K_S$  invariant mass  $m_{12}$  is plotted along the horizontal axis, and the  $K_S p$  invariant mass  $m_{23}$  is plotted along the vertical axis (note the linear scale). The strips show the positions of the  $\phi$  and  $\Theta^+$  resonances. The  $\Theta$ – $\phi$  interference occurs at the intersection of the strips, thus within the range of  $E_\gamma$  from 1.74 to 2.15 GeV (bottom).

Energies below 1.74 GeV are too small to produce the  $\Theta^+$  resonance (whose mass we assume equal 1537 MeV); at energies above 2.25 GeV the decay products of  $\Theta^+$  and  $\phi$  do not overlap, hence there is no interference.

### C. A sum of two Breit–Wigner’s

In the  $\gamma p \rightarrow K_L K_S p$  amplitude, there are two rapidly varying functions: one is the  $\phi$  resonance pole in the invariant variable  $m_{12}$  and the other is the  $\Theta^+$  resonance pole in the invariant variable  $m_{23}$ . The corresponding widths,  $\Gamma_\phi = 4.26$  MeV and  $\Gamma_\Theta \sim 0.5$  MeV, are very small as compared to the typical hadron masses of several hundred MeV which define the scale of variation of other factors in the amplitude. Therefore, we can write the

fast varying pieces of the amplitude without knowing the detailed dynamics of the process. It is a coherent sum of two Breit–Wigner amplitudes in the variables  $m_{12}$  and  $m_{23}$ , times slowly varying factors:

$$\mathcal{A} = A_\phi \frac{\sqrt{\Gamma_\phi}}{m_{12} - m_\phi + i\frac{\Gamma_\phi}{2}} + A_\Theta \frac{\sqrt{\Gamma_\Theta}}{m_{23} - m_\Theta + i\frac{\Gamma_\Theta}{2}} + B \quad (1)$$

where  $A_{\phi,\Theta}$  are the  $\phi, \Theta$  resonance production amplitudes which are, generally, functions of all kinematical invariants but are slowly varying on the scale of  $\Gamma_{\phi,\Theta}$ . Having a dynamical model for the resonance production these amplitudes can be computed. We shall, however, attempt to extract as much information from eq. (1) as possible without knowing their detailed form. We have added a non-resonance amplitude  $B$  which does not contain the  $s$ -channel resonances and hence is also a slowly varying function of  $m_{12}$  and  $m_{23}$ .  $A_{\phi,\Theta}$  and  $B$  are generally complex. We introduce the ratios

$$\frac{A_\Theta}{A_\phi} := R e^{i\delta}, \quad \frac{B}{A_\phi} := \rho e^{i\eta}. \quad (2)$$

To shorten equations, we introduce also the shifts of invariant masses from their resonance positions:

$$\Delta_\phi := 2(m_{12} - m_\phi), \quad \Delta_\Theta := 2(m_{23} - m_\Theta). \quad (3)$$

The cross section is proportional to  $|\mathcal{A}|^2$  which we write as

$$\begin{aligned} \sigma(m_{12}, m_{23}, \dots) = & |C|^2 \left[ \frac{\Gamma_\phi}{\Delta_\phi^2 + \Gamma_\phi^2} + R^2 \frac{\Gamma_\Theta}{\Delta_\Theta^2 + \Gamma_\Theta^2} + \frac{\rho^2}{4} \right. \\ & + 2R\sqrt{\Gamma_\phi\Gamma_\Theta} \frac{(\Delta_\phi\Delta_\Theta + \Gamma_\phi\Gamma_\Theta) \cos \delta + (\Delta_\phi\Gamma_\Theta - \Gamma_\phi\Delta_\Theta) \sin \delta}{(\Delta_\phi^2 + \Gamma_\phi^2)(\Delta_\Theta^2 + \Gamma_\Theta^2)} \\ & + \rho\sqrt{\Gamma_\phi} \frac{\Delta_\phi \cos \eta - \Gamma_\phi \sin \eta}{\Delta_\phi^2 + \Gamma_\phi^2} \\ & \left. + R\rho\sqrt{\Gamma_\Theta} \frac{\Delta_\Theta \cos(\eta - \delta) - \Gamma_\Theta \sin(\eta - \delta)}{\Delta_\Theta^2 + \Gamma_\Theta^2} \right]. \quad (4) \end{aligned}$$

The first term is the square of the  $\phi$  resonance production amplitude, the second term is the square of the  $\Theta$  resonance production amplitude (suppressed by the *square* of the small ratio of the two amplitudes  $R^2 \ll 1$ ), the third term is the non-resonant contribution. In principle, one has to add to it a possible non-coherent non-resonant contribution but such terms will be irrelevant for our procedure, below.

The most interesting term is the second line in eq. (4): it gives the interference between the  $\phi$  and  $\Theta$  resonance amplitudes. The third and fourth lines are the interference terms of  $\phi$  and  $\Theta$  respectively with the non-resonant amplitudes. These terms are non-negligible along the resonance strips in Fig. 2. The interference term in the second line is essential at the intersection of those strips. Let us discuss it in more detail.

First of all, it is linear in the  $\Theta$  production amplitude  $R$  (relative to that of the  $\phi$  production); at  $R \ll 1$  it may be much larger than the incoherent  $\Theta^+$  production. To get an idea how small  $R$  is we estimate it roughly from the ratio of the  $\phi$  and  $\Theta$  photoproduction. The first is about  $3 \mu\text{b}$  at  $E_\gamma \approx 2 \text{ GeV}$  and the second is about  $0.2 \text{ nb}$  [10], which gives an estimate  $R^2 \sim 1/1500$ ,  $R \sim 1/40$ .

Second, the interference term is proportional to  $\sqrt{\Gamma_\phi\Gamma_\Theta}$ . It reflects the fact that if one (or both) of the interfering resonances is almost stable ( $\Gamma \rightarrow 0$ ), its decay products are carried out far away from the reaction vertex, and there is no interference.

Most important, if one looks for the events where the  $K_L K_S$  mass  $m_{12}$  is within the  $\phi$  resonance width, meaning  $\Delta_\phi \sim \Gamma_\phi$ , and where the  $K_S p$  mass  $m_{23}$  is within the  $\Theta^+$  width, meaning  $\Delta_\Theta \sim \Gamma_\Theta$ , the interference term is of the order  $R/(\sqrt{\Gamma_\phi\Gamma_\Theta})$  which may be quite large despite the smallness of the production rate  $R$ . It is helpful that  $\phi$  is a narrow resonance.

The interference term in the second line of eq. (4) depends essentially on the relative phase  $\delta$  of the  $\phi$  and  $\Theta^+$  production amplitudes. Can anything be said about  $\delta$  without going into a detailed dynamical model for the amplitudes? As we argued in the Introduction, the  $\Theta^+$  production amplitude (Fig. 1, left) is dominated by the Reggeized  $K^*$  exchange [10]. At low energies  $E_\gamma \sim 2 \text{ GeV}$  we are interested in, the effect of the Reggeization is not large and it can be fairly well replaced by the usual  $K^*$  meson exchange. The amplitude  $A_\Theta$  is then real. As to the photoproduction of  $\phi$  (Fig. 1, right), it is notoriously complicated at  $E_\gamma \sim 2 \text{ GeV}$ , with no single dominating mechanism [24]. It may be a mixture of Pomeron,  $\pi^0, \eta$  and other meson exchanges. Out of these, only the diffractive Pomeron amplitude is nearly purely imaginary as it is the “shadow” from the total  $\gamma p$  cross section with many particles produced, at least at high energies where the Pomeron exchange dominates. At  $2 \text{ GeV}$ , however, the  $\phi$  photoproduction is still far from its asymptotics at high energies [24] and hence the Pomeron exchange cannot dominate. Therefore, we expect that the amplitude  $A_\phi$  is nearly real, too. We, thus, expect the relative phase  $\delta \approx 0$  in the energy range of interest. Non-zero values of  $\delta$  are, however, not excluded until measured directly.

Putting for simplicity  $\delta = 0$  in eq. (4) we see that the  $\phi - \Theta$  interference term is proportional to

$$\sigma_{\text{interf}} \sim \frac{\Delta_\phi\Delta_\Theta + \Gamma_\phi\Gamma_\Theta}{(\Delta_\phi^2 + \Gamma_\phi^2)(\Delta_\Theta^2 + \Gamma_\Theta^2)}. \quad (5)$$

We note that the interference term falls off as  $1/\Delta_\phi\Delta_\Theta$  at large distances from the resonances positions and it is maximal when  $m_{12} \approx m_\phi$  and  $m_{23} \approx m_\Theta$ , *i.e.* near the intersection of the two resonance strips on the Dalitz plot of Fig. 2. The r.h.s. of eq. (5) is positive when both  $\Delta_\phi$  and  $\Delta_\Theta$  have the same sign, *i.e.* when the invariant masses  $m_{12}$  and  $m_{23}$  are both above or both below the centers of the resonances. It means seeing more events in the upper right and lower left corners of the intersection of two resonance strips. When  $\Delta_\phi$  and  $\Delta_\Theta$  have opposite

signs, the interference term may become negative, meaning seeing less events in the upper left and lower right corners. This “checker board” pattern of events is illustrated in Fig. 3a where eq. (5) is plotted in the  $(\Delta_\phi, \Delta_\Theta)$  axes measured in units of the corresponding widths. Although we gave an argument that in this case  $\delta \approx 0$  we also plot in Fig. 3 the excess/deficiency of the number of events from the interference term in eq. (4) for other values of the relative phase  $\delta = \frac{\pi}{2}, -\frac{\pi}{2}$  and  $\pi$ .

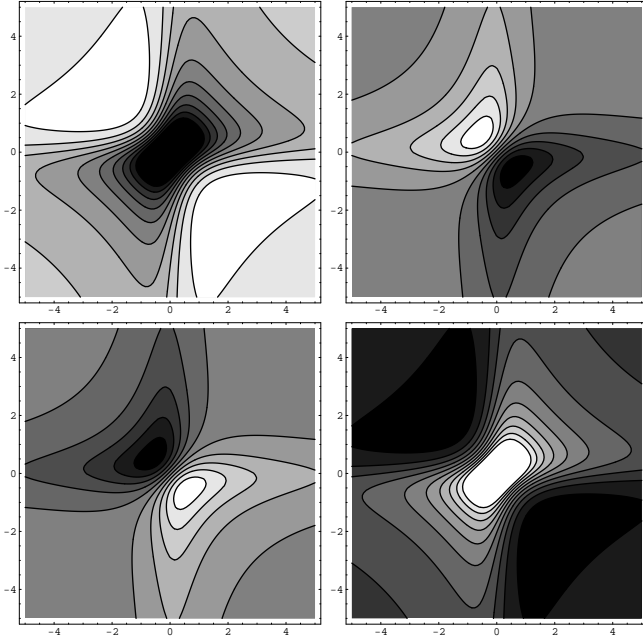


FIG. 3: The excess/deficiency of events on the  $(m_{12}, m_{23})$  Dalitz plot around the centers of both resonances, at various values of the relative phase  $\delta = 0, \frac{\pi}{2}, -\frac{\pi}{2}, \pi$ . These are contour plots with the excess events shown darker and the deficiency of events shown lighter.

The difference in the event pattern is so strong that one would be probably able to say from the first glance on the Dalitz plot what is the relative phase.

### III. TAILORING OUT THE $\Theta^+$ RESONANCE

The cross section of the  $\gamma p \rightarrow K_L K_S p$  reaction (4) can be divided into terms even and odd with respect to  $\Delta_\phi$ , meaning terms even and odd with respect to the reflection about the  $m_{12} = m_\phi$  axis (the vertical strip in Fig. 2). More interesting information on  $\Theta^+$  contains in the *odd* part. To extract it, we integrate all events in some range of  $m_{12}$  from the center of the  $\phi$  resonance  $m_\phi$  up to some  $m_\phi + \mu_\phi$  and *subtract* all events integrated symmetrically below the resonance center, from  $m_\phi - \mu_\phi$  to  $m_\phi$ . The smaller limit  $\mu_\phi$  theoretically the cleaner, however one has to make a compromise with the statistics. Probably, integrating over the resonance within a few units of its width is optimal. On the one hand, most of the events in the  $\phi$  resonance range will be collected

and on the other hand, the integration strip will be still narrow enough to neglect the dependence of other, non-resonance factors on  $m_{12}$ .

As the result of this subtraction of events, most terms in eq. (4) cancel out, most notably the background which is a smooth function at  $m_{12} \approx m_\phi$ , and the large square of the  $\phi$  production amplitude (the first term in eq. (4)). We obtain:

$$\begin{aligned} & \int_{m_\phi - \mu_\phi}^{m_\phi + \mu_\phi} dm_{12} \sigma(m_{12}, m_{23}) - \int_{m_\phi - \mu_\phi}^{m_\phi} dm_{12} \sigma(m_{12}, m_{23}) \\ &= \frac{1}{2} \ln \left[ 1 + \left( \frac{2\mu_\phi}{\Gamma_\phi} \right)^2 \right] \\ & \times |C|^2 \sqrt{\Gamma_\phi} \left( 2R\sqrt{\Gamma_\Theta} \frac{\Delta_\Theta \cos \delta + \Gamma_\Theta \sin \delta}{\Delta_\Theta^2 + \Gamma_\Theta^2} + \rho \cos \eta \right). \end{aligned} \quad (6)$$

(we have retained a non-zero  $\delta$  for generality).

Eq. (6) exhibits a  $\Theta^+$  resonance term originating from the interference, and a non-resonant background. Analysis based on eq. (6) has a clear advantage over a resonance search based on standard technique. First, the signal is linear (and not quadratic) in the small production amplitude  $R$ , second, most of the parasitic background is canceled by the symmetric subtraction procedure. Third, the only background left is due to the *coherent* non-resonant production which is not expected to be large in this case. Fourth, the resonance has a definite oscillating signature. As we shall see in the next section, it is not likely that this signature is blurred out by the finite experimental errors.

### IV. SMEARING WITH THE EXPERIMENTAL RESOLUTION

The above equations have been written for an idealized case, assuming the experimental resolution is perfect. Actually, it never is. Assuming eq. (4) is written for the ‘true’ values of the variables  $m_{12}^{\text{true}}, m_{23}^{\text{true}}$  one has to smear it with the probability distribution that the measured  $m_{12}^{\text{obs}}, m_{23}^{\text{obs}}$  deviate from the true ones. We shall assume that the errors in measuring the invariant masses  $m_{12}^{\text{obs}}$  and  $m_{23}^{\text{obs}}$  are statistically independent and that the error probability distribution is given by the product of two Gaussian functions with equal widths  $\sigma$ :

$$\frac{\exp \left( -\frac{(m_{12}^{\text{obs}} - m_{12}^{\text{true}})^2}{2\sigma^2} \right)}{\sqrt{2\pi\sigma^2}} \cdot \frac{\exp \left( -\frac{(m_{23}^{\text{obs}} - m_{23}^{\text{true}})^2}{2\sigma^2} \right)}{\sqrt{2\pi\sigma^2}}. \quad (7)$$

To be concrete, we take the mean square error in measuring  $m_{12}, m_{23}$  to be  $\sigma = 5$  MeV. If a more realistic error distribution function is known it should be used instead of eq. (7).

To get the observable cross section as function of  $m_{12}^{\text{obs}}$  and  $m_{23}^{\text{obs}}$ , one has to integrate the theoretical eq. (4) understood as function of  $m_{12}^{\text{true}}$  and  $m_{23}^{\text{true}}$ , over these variables with the error weight (7). In eq. (4) there are two

kind of functions encountered: one is symmetric with respect to the resonance center, the other is antisymmetric. We introduce their smeared counterparts:

$$\frac{\Gamma}{\Delta^2 + \Gamma^2} \rightarrow \int dm^{\text{true}} \frac{\exp\left(-\frac{(m^{\text{obs}} - m^{\text{true}})^2}{2\sigma^2}\right)}{\sqrt{2\pi\sigma^2}} \quad (8)$$

$$\times \frac{\Gamma}{4(m^{\text{true}} - m^{\text{res}})^2 + \Gamma^2} := G(m^{\text{obs}} - m^{\text{res}}, \Gamma, \sigma),$$

$$\frac{\Delta}{\Delta^2 + \Gamma^2} \rightarrow \int dm^{\text{true}} \frac{\exp\left(-\frac{(m^{\text{obs}} - m^{\text{true}})^2}{2\sigma^2}\right)}{\sqrt{2\pi\sigma^2}} \quad (9)$$

$$\times \frac{2(m^{\text{true}} - m^{\text{res}})}{4(m^{\text{true}} - m^{\text{res}})^2 + \Gamma^2} := D(m^{\text{obs}} - m^{\text{res}}, \Gamma, \sigma).$$

The smeared functions  $G$  and  $D$  are even (odd) in  $m^{\text{obs}} - m^{\text{res}}$ , respectively. If the resonance is much more narrow than the experimental resolution ( $\Gamma \ll \sigma$  – this is the case of the  $\Theta^+$  resonance) the two functions are analytically computable:

$$G(\Delta m, \Gamma, \sigma) \stackrel{\Gamma \ll \sigma}{\approx} \frac{\pi}{2\sqrt{2\pi\sigma^2}} \exp\left(-\frac{(\Delta m)^2}{2\sigma^2}\right), \quad (10)$$

$$D(\Delta m, \Gamma, \sigma) \stackrel{\Gamma \ll \sigma}{\approx} \frac{\pi}{2\sqrt{2\pi\sigma^2}} \exp\left(-\frac{(\Delta m)^2}{2\sigma^2}\right) \cdot \text{sign}(\Delta m) \text{Erfi}\left(\frac{\Delta m}{\sqrt{2\sigma^2}}\right) \quad (11)$$

where Erfi is the error function of imaginary argument,

$$\text{Erfi}(z) = -i \text{Erf}(iz) = -i \frac{2}{\sqrt{\pi}} \int_0^{iz} dt e^{-t^2}.$$

The two functions  $G(\Delta m)$  and  $D(\Delta m)$  are plotted in Fig. 4.

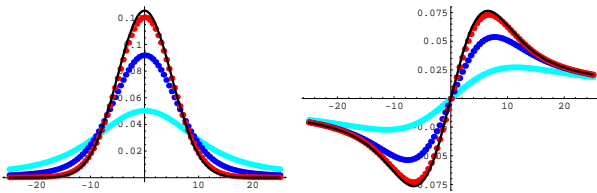


FIG. 4: The resonance functions smeared with a Gaussian error distribution,  $\sigma = 5$  MeV: the symmetric function  $G$  (left) and the antisymmetric function  $D$  (right). The red curve corresponds to smearing the  $\Theta^+$  resonance assuming  $\Gamma_\Theta = 0.5$  MeV, the blue curve shows the smearing of  $\phi$ ,  $\Gamma_\phi = 4.26$  MeV, and the light blue curve shows the smearing of the  $\Lambda(1520)$  resonance,  $\Gamma_\Lambda = 15.6$  MeV. Solid curves are the asymptotic  $G, D$  functions ( $\Gamma \rightarrow 0$ ). The distance to the resonance  $\Delta m$  is plotted along the horizontal axis, in MeV. Note that smearing of the  $\Theta^+$  resonance is well described by the asymptotic functions (10,11).

It is now easy to write down the cross section resulting from smearing eq. (4) with the experimental resolution.

One has simply to replace the corresponding factors in eq. (4) by

$$\begin{aligned} \frac{\Gamma_\phi}{\Delta_\phi^2 + \Gamma_\phi^2} &\rightarrow G(m_{12} - m_\phi, \Gamma_\phi, \sigma), \\ \frac{\Delta_\phi}{\Delta_\phi^2 + \Gamma_\phi^2} &\rightarrow D(m_{12} - m_\phi, \Gamma_\phi, \sigma), \\ \frac{\Gamma_\Theta}{\Delta_\Theta^2 + \Gamma_\Theta^2} &\rightarrow G(m_{23} - m_\Theta, \Gamma_\Theta, \sigma), \\ \frac{\Delta_\Theta}{\Delta_\Theta^2 + \Gamma_\Theta^2} &\rightarrow D(m_{23} - m_\Theta, \Gamma_\Theta, \sigma). \end{aligned}$$

All four functions are plotted in Fig. 4. The same replacement should be done in the  $\phi$ – $\Theta$  interference term, eq. (5), which becomes, after smearing,

$$\begin{aligned} \sigma_{\text{interf}} &\sim D(m_{12} - m_\phi, \Gamma_\phi, \sigma) D(m_{23} - m_\Theta, \Gamma_\Theta, \sigma) \\ &+ G(m_{12} - m_\phi, \Gamma_\phi, \sigma) G(m_{23} - m_\Theta, \Gamma_\Theta, \sigma). \end{aligned} \quad (12)$$

Its contour plot is shown in Fig. 5. Comparing it with the plot in Fig. 3, left, we observe that the ‘checker-board’ pattern of the interference is preserved by the finite experimental resolution. [It should be reminded however, that the simple result (12) has been obtained assuming that the errors in measuring the invariant ( $K_L K_S$ ) and ( $K_S p$ ) masses are statistically independent. Whether it is indeed a fair approximation needs a special study.]

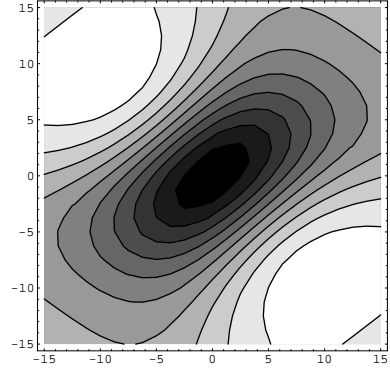


FIG. 5: Contour plot for the excess/deficiency of events smeared with the experimental resolution of 5 MeV, which is due to the  $\phi$ – $\Theta$  interference, eq. (12). The excess is shown darker and the deficiency shown lighter.  $m_{12} - m_\phi$  is plotted along the horizontal axis, and  $m_{23} - m_\Theta$  is plotted along the vertical axis, both in MeV. The relative phase  $\delta$  is assumed to be zero.

We can now virtually apply the  $\Theta^+$  identifying procedure described in Section III. Namely, we integrate all events with  $m_{12}$  from the center of the  $\phi$  resonance  $m_\phi$  up to some  $m_\phi + \mu_\phi$ , and *subtract* events integrated from  $m_\phi - \mu_\phi$  to  $m_\phi$ . This procedure nullifies all terms that are symmetric with respect to the center of the  $\phi$  and stresses terms that are antisymmetric, in particular the

interference term:

$$\begin{aligned} & \int_{m_\phi}^{m_\phi + \mu_\phi} dm_{12} \sigma(m_{12}, m_{23}) - \int_{m_\phi - \mu_\phi}^{m_\phi} dm_{12} \sigma(m_{12}, m_{23}) \\ &= \text{const.} \left\{ 2R\sqrt{\Gamma_\Theta} [D(m_{23} - m_\Theta, \Gamma_\Theta, \sigma) \cos \delta \right. \\ & \quad \left. + G(m_{23} - m_\Theta, \Gamma_\Theta, \sigma) \sin \delta] + \rho \cos \eta \right\}. \end{aligned} \quad (13)$$

Apart from a smooth background term  $\rho \cos \eta$ , eq. (13) exhibits a characteristic behavior associated with the  $\Theta^+$ . If the relative phase  $\delta \approx 0$  (as we think it is) only the  $D$ -function antisymmetric with respect to the  $\Theta^+$  resonance center survives in eq. (13); its plot is presented in Fig. 4, right, and is in fact very close to the asymptotic eq. (11). Fitting the difference in the integrated cross section about the  $\phi$  resonance by eq. (13) it is possible to find the position of the  $\Theta^+$  resonance: it is where the function  $D(m_{23} - m_\Theta)$  changes sign.

Determining the value of the width  $\Gamma_\Theta$  is more difficult, especially if the relative phase  $\delta \approx 0$ . Nevertheless, the shape of the  $D(m_{23} - m_\Theta)$  curve depends implicitly on the width even if  $\Gamma_\Theta$  is less than the experimental resolution  $\sigma$ , as seen from the comparison of the curves for  $\Gamma = 0.5 \text{ MeV}$  and  $4 \text{ MeV}$  in Fig. 4, right. Depending on the quality of the data, one would be probably able to establish from data fitting that  $\Gamma_\Theta$  is less than a few MeV which would be anyway a record achievement.

## V. TRIPLE INTERFERENCE

The reaction  $\gamma p \rightarrow K_S K_L p$  at  $E_\gamma \sim 2 \text{ GeV}$  is unique in that all three pairs of the final particles resonate, and those resonances can interfere when the final states overlap. Resonance interference can occur when any two of the invariant masses  $m_{12} \equiv m(K_L K_S)$ ,  $m_{13} \equiv m(K_L p)$ ,  $m_{23} \equiv m(K_S p)$ , are close to the resonance masses  $m_\phi$ ,  $m_\Theta$ ,  $m_\Theta$ , respectively, see Fig. 6. In fact the distribution in the  $m_{13}$  invariant mass has been also studied in the same experiment [7] where only an upper limit for the  $\Theta^+$  production has been established.

Everything said above about the  $\phi$ - $\Theta$  interference in the  $m_{12}$ - $m_{23}$  Dalitz plot can be immediately translated into the  $\phi$ - $\Theta$  interference in the  $m_{12}$ - $m_{13}$  axes. One can apply the event-subtraction method described in the previous section: it results in the same eq. (13), with  $m_{23}$  replaced by  $m_{13}$ . This seems to be a rather cheap way of approximately doubling the statistics used to analyze eq. (13).

Another possibility is to look, at  $E_\gamma \geq 1.85 \text{ GeV}$ , for the interference of the  $\Theta^+$  decay into  $K_S p$  vs its decay into  $K_L p$ . Introducing the shifts of the invariant masses from the resonance center,  $\Delta_\Theta = 2(m_{23} - m_\Theta)$ ,  $\Delta'_\Theta = 2(m_{13} - m_\Theta)$ , one writes the coherent  $\Theta^+$  production

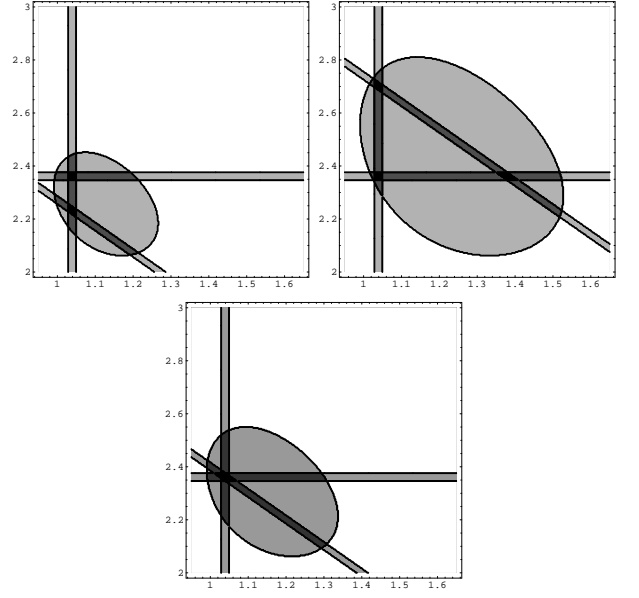


FIG. 6: Phase volumes (Dalitz plots) for the  $\gamma p \rightarrow K_L K_S p$  reaction at photon lab energies  $E_\gamma = 1.80, 2.05$  and  $1.87 \text{ GeV}$ . The  $K_L K_S$  invariant mass squared  $m_{12}^2$  is plotted along the horizontal axis, and the  $K_S p$  invariant mass squared  $m_{23}^2$  is plotted along the vertical axis. The strips show the  $\phi(K_L K_S)$ ,  $\Theta(K_S p)$  and  $\Theta(K_L p)$  resonances. Resonance interference occurs at the intersection of the strips; at  $E_\gamma = 1.87 \text{ GeV}$  all three resonances interfere (bottom).

cross section at small  $\Delta_\Theta, \Delta'_\Theta$  as

$$\begin{aligned} \sigma^{\Theta\Theta} &\sim \Gamma_\Theta \left[ \frac{|A_\Theta|^2}{\Delta_\Theta^2 + \Gamma_\Theta^2} + \frac{|A'_\Theta|^2}{\Delta'^2_\Theta + \Gamma_\Theta^2} \right. \\ &\quad \left. - 2 \frac{|A_\Theta||A'_\Theta|(\Delta_\Theta \Delta'_\Theta + \Gamma_\Theta^2)}{(\Delta_\Theta^2 + \Gamma_\Theta^2)(\Delta'^2_\Theta + \Gamma_\Theta^2)} \right] \end{aligned} \quad (14)$$

where the first two terms stand for the incoherent  $\Theta^+$  production observed through the  $K_S p$  and  $K_L p$  channels, respectively, and the third term is their interference.  $A_\Theta, A'_\Theta$  are the production amplitudes which are, generally, functions of the invariants but can be replaced by constants when  $m(K_S p), m(K_L p) \approx m_\Theta$ . In the ideal geometry case  $|A_\Theta| = |A'_\Theta|$ , however the experimental acceptance may violate this symmetry.

In this case interference is not amplified by the large  $\phi$  production amplitude and all terms are quadratic in the  $\Theta^+$  production amplitude. After smearing with the experimental resolution (Section IV) the effect of interference becomes insignificant. Nevertheless, it might be helpful to make a Dalitz plot of the events in the  $m_{13}$ - $m_{23}$  axes: at the intersection of the  $m(K_S p) \approx m_\Theta$ ,  $m(K_L p) \approx m_\Theta$  strips there can be more events associated with the  $\Theta^+$  production than one can discriminate in the separate  $K_S p$  and  $K_L p$  mass spectra.

Finally, the most non-trivial *triple* interference happens at  $E_\gamma \approx 1.87 \text{ GeV}$  where all three resonance strips cross at one point, see Fig. 6, bottom. Keeping only

the presumably largest terms linear in the  $\Theta^+$  production amplitudes, one generalizes the second line term in eq. (4) to include interference between the  $\phi$  meson and the two  $\Theta$ 's, one decaying into  $K_S p$  and the other into  $K_L p$ :

$$\begin{aligned} \sigma^{\phi\Theta\Theta} = & 2|C|^2 \frac{\sqrt{\Gamma_\phi \Gamma_\Theta}}{\Delta_\phi^2 + \Gamma_\phi^2} \\ & \cdot \left[ \left( R \frac{\Delta_\phi \Delta_\Theta + \Gamma_\phi \Gamma_\Theta}{\Delta_\Theta^2 + \Gamma_\Theta^2} + R' \frac{\Delta_\phi \Delta'_\Theta + \Gamma_\phi \Gamma_\Theta}{\Delta_\Theta'^2 + \Gamma_\Theta^2} \right) \cos \delta \right. \\ & \left. + \left( R \frac{\Delta_\phi \Gamma_\Theta - \Gamma_\phi \Delta_\Theta}{\Delta_\Theta^2 + \Gamma_\Theta^2} + R' \frac{\Delta_\phi \Gamma_\Theta - \Gamma_\phi \Delta'_\Theta}{\Delta_\Theta'^2 + \Gamma_\Theta^2} \right) \sin \delta \right]. \end{aligned} \quad (15)$$

The three pairs' invariant masses are constrained by  $m_{12}^2 + m_{13}^2 + m_{23}^2 = s + 2m_{K^0}^2 + m_p^2$ , hence the three small deviations from the resonance centers are constrained by

$$\Delta_\Theta m_\Theta + \Delta'_\Theta m_\Theta + \Delta_\phi m_\phi = \Delta_\gamma m_p \quad (16)$$

where  $\Delta_\gamma$  is the (doubled) deviation of the photon lab energy from 1.87 GeV where all three resonance strips cross at one point in the Dalitz plot:

$$\Delta_\gamma := 2(E_\gamma - E_\gamma^{(3)}), \quad (17)$$

$$E_\gamma^{(3)} := \frac{2m_\Theta^2 + m_\phi^2 - 2m_{K^0}^2 - m_p^2}{2m_p} \approx 1.87 \text{ GeV}.$$

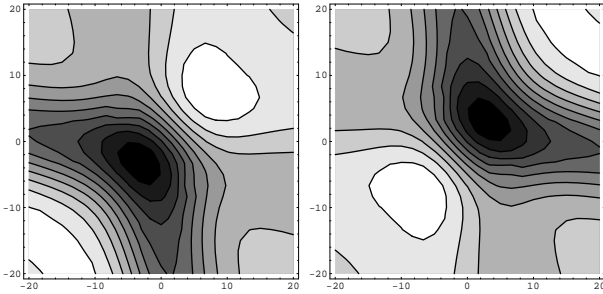


FIG. 7: Triple  $\phi - \Theta(K_S p) - \Theta(K_L p)$  interference pattern from eq. (15), plotted in the  $m_{13} = m(K_L p)$  (horizontal) and  $m_{23} = m(K_S p)$  (vertical) axes, in MeV. The axes' zeroes correspond to  $m_{13} = m_{23} = m_\Theta$ . The left panel shows the excess (darker) and deficiency (lighter) of events integrated over the range of  $E_\gamma$  from 1.82 to 1.87 GeV, smeared with the experimental resolution of 5 MeV. The right panel shows the events integrated over the range of  $E_\gamma$  from 1.87 to 1.92 GeV. The relative phase  $\delta$  of the  $\phi$  and  $\Theta^+$  production amplitudes is assumed to be zero.

Note that, although the  $\Theta$  amplitude is antisymmetric under the interchange of  $K_S \leftrightarrow K_L$ , so is the  $\phi$  amplitude, therefore the interference cross section is symmetric, hence the relative plus sign in the  $R, R'$  terms. In the ideal acceptance case the ratios of the production amplitudes are equal,  $R = R'$ . In reality, however, these ratios

may appear to be non-equal owing to different ways one registers  $K_S, K_L$ .

Eq. (15) predicts a rich structure of event density in the Dalitz plot near the triple interference point at  $E_\gamma \approx 1.87$  GeV, which, however, needs to be smeared by the experimental resolution. We assume that errors in measuring the invariant masses  $m_{13}$  and  $m_{23}$  are statistically independent and are given by the Gaussian distributions with dispersion  $\sigma$  which we take equal 5 MeV. The interference pattern survives smearing: it is presented in Fig. 7 which demonstrates a striking asymmetry between event patterns above the energy  $E_\gamma = 1.87$  GeV, and below it.

Another way to stress the interference phenomenon (and also to reduce considerably the background) is to integrate events in the upper right corner of Fig. 7 and *subtract* events in the lower left corner, as function of the incident photon energy. The resulting excess/deficiency as function of  $E_\gamma$  is shown in Fig. 8.

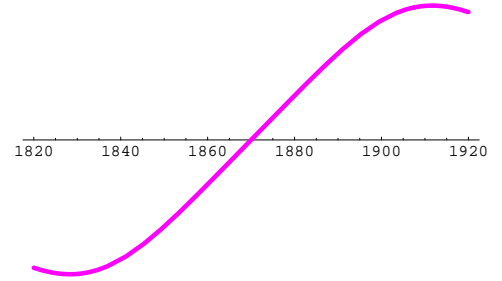


FIG. 8: Triple  $\phi - \Theta(K_S p) - \Theta(K_L p)$  interference: number of events with  $m_{13}, m_{23} < m_\Theta$  subtracted from the number of events with  $m_{13}, m_{23} > m_\Theta$ , as function of the photon lab energy  $E_\gamma$ , in MeV.

Using eq. (15) one can extract other peculiar characteristics of the unique triple interference in the  $\gamma p \rightarrow K_L K_S p$  reaction.

## VI. $\Theta^+$ INTERFERENCE WITH $\Lambda(1520)$

Interference can be probably observed also in the  $\gamma p \rightarrow K^+ \Lambda(1520) \rightarrow K^+ (\bar{K}^0 n)$  reaction at photon lab energies  $E_\gamma$  between 1.81 and 2.17 GeV where the final state can interfere with the same final state from the  $\gamma p \rightarrow \bar{K}^0 \Theta^+ \rightarrow \bar{K}^0 (K^+ n)$  reaction, see the phase volume plots in Fig. 9.

This reaction has been studied in the same experiment [7], also with a null result for the  $\Theta^+$  search. There were many final states found identified with the  $\bar{K}^0 n$  decay of the  $\Lambda(1520)$  resonance, however they were cut out from the analysis [7]. We suggest that precisely these events should be analyzed with respect to the possible interference with the  $\Theta^+$  production. The procedure to isolate the interference term is exactly as described above for the case of the  $\phi$  meson, the only difference being that  $\Lambda(1520)$  has the width larger than that of  $\phi$ ,



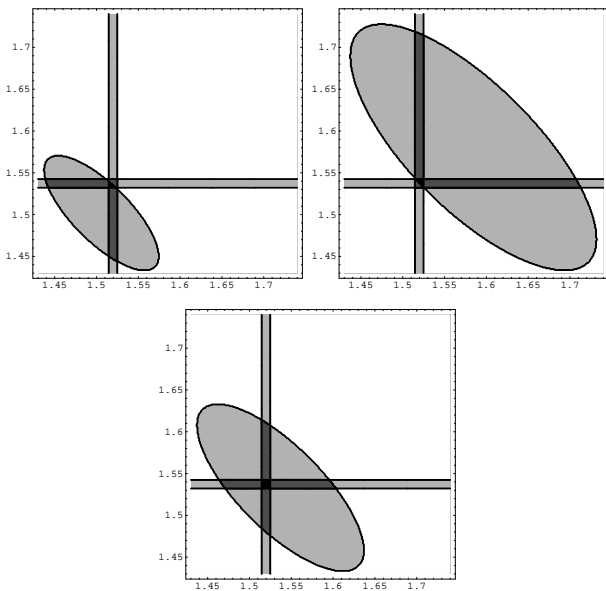


FIG. 9: Phase volumes (Dalitz plots) for the  $\gamma p \rightarrow \bar{K}^0 K^+ n$  reaction at photon lab energies  $E_\gamma = 1.81, 2.17$  and  $1.95$  GeV. The  $\bar{K}^0 n$  invariant mass  $m_{12}$  is plotted along the horizontal axis, and the  $K^+ n$  invariant mass  $m_{23}$  is plotted along the vertical axis (note the linear scale). The strips show the positions of the  $\Lambda(1520)$  and  $\Theta^+$  resonances ( $m_\Theta = 1537$  MeV is assumed). The  $\Theta$ - $\Lambda$  interference occurs at the intersection of the strips, thus within the range of  $E_\gamma$  from  $1.81$  to  $2.17$  GeV.

$\Gamma_\Lambda = 15.6$  MeV, therefore the interference picture may be less pronounced. However,  $\Gamma_\Lambda$  is still much less than the typical hadron masses determining the scale of variation of the production amplitudes, therefore one may hope that the equations of the previous Sections apply to this case as well. In particular, subtracting events slightly below the  $\Lambda$  resonance from those slightly above, should result in the same eq. (13) exhibiting an oscillating behavior in the  $(K^+ n)$  invariant mass (but with a different background contribution denoted in eq. (13) as  $\rho \cos \eta$ ). The excess/deficiency of events due to the  $\Theta$ - $\Lambda$  interference is shown in Fig. 10 which is similar to Fig. 5.

## VII. CONCLUSIONS

Lately, strong signals of the exotic  $\Theta^+$  baryon have been observed in the direct formation experiment by the DIANA collaboration [13] and in a quasi-formation experiment by the LEPS collaboration [12]. The results from numerous production experiments are still controversial, the main reason being the small couplings of  $\Theta^+$  with ordinary hadrons. The origin of those small couplings are theoretically well understood (see a recent brief review in Ref. [11]), however they preclude an easy observation of the  $\Theta^+$  in most of the production experiments.

To override the smallness of the  $\Theta^+$  production cross sections, a new way of  $\Theta^+$  searching is suggested, based

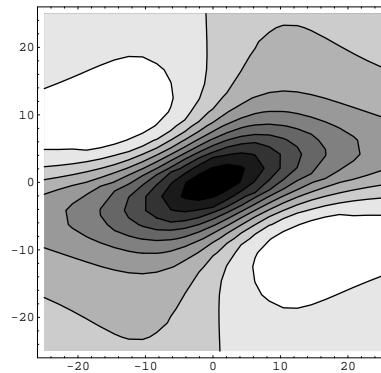


FIG. 10: Contour plot for the excess/deficiency of events smeared with the experimental resolution of  $5$  MeV, which is due to the  $\Lambda(1520)$ - $\Theta$  interference, eq. (12). The excess is shown darker and the deficiency shown lighter.  $m(\bar{K}^0 n) - m_\Lambda$  is plotted along the horizontal axis, and  $m(K^+ n) - m_\Theta$  is plotted along the vertical axis, both in MeV. The relative phase  $\delta$  of the two production amplitudes is assumed to be zero.

on the interference between the small  $\Theta^+$  production amplitude and the large production amplitude of a known resonance yielding the same final state. Owing to the narrowness of the resonances, a model-independent coherent sum of the two resonance amplitudes can be applied giving an unambiguous interference term. The interference may be substantial in the kinematical range where the invariant masses of the resonances' decay products are close to the resonances' centers. The pattern of events due to interference allows to determine the relative phase of the two resonance amplitudes.

We have suggested a procedure for the analysis of the interference, based on the *subtraction* of events above and below one of the resonances, to purify the signature of the other one and to get rid of a large, if not dominant, part of the background. Smearing by a finite experimental resolution is not likely to blur out the characteristic oscillating nature of the resulting event pattern. With sufficient statistics, the mass of the  $\Theta^+$  resonance can be accurately established and a tight upper limit for its width determined.

The method is directly applicable to the  $\gamma p \rightarrow \bar{K}^0 K^0 p$  and  $\bar{K}^0 K^+ n$  reactions at relatively low energies, studied in a recent CLAS experiment. In the first case one should look for the  $\Theta - \phi$  and in the second case for the  $\Theta - \Lambda(1520)$  interference. In the first reaction also a unique *triple* interference can be examined at a particular photon energy  $E_\gamma \approx 1.87$  GeV.

The suggested method of studying  $\Theta^+$  production through interference is applicable to other experiments, wherever the  $\Theta^+$  can kinematically interfere with a known resonance whose production rate is large.



## Acknowledgements

We are grateful to Ya. Azimov, V. Petrov and A. Titov for useful discussions. The work of M.A. is supported by the US DOE grant FG02-96ER40960. D.D. acknowledges support by the A.v.Humboldt Research Award during the visit to Bochum University. D.D.'s work is supported

in part by Russian Government grants 1124.2003.2 and RFBR 06-02-16786. M.P. is supported by the Sofja Kowalewskaja Programme of the A.v.Humboldt Foundation, by German Federal Ministry for Education and Research (BMBF), and DFG grant SFB TR-16.

- 
- [1] T. Nakano [LEPS Collaboration], Talk at the PANIC 2002 (Oct. 3, 2002, Osaka); T. Nakano *et al.*, Phys. Rev. Lett. **91**, 012002 (2003), arXiv: hep-ex/0301020.
  - [2] V.A. Shebanov [DIANA Collaboration], Talk at the Session of the Nuclear Physics Division of the Russian Academy of Sciences (Dec. 3, 2002, Moscow); V.V. Barmin *et al.*, Phys. Atom. Nucl. **66**, 1715 (2003) [Yad. Fiz. **66**, 1763 (2003)], arXiv: hep-ex/0304040.
  - [3] The two experiments were totally independent as both groups didn't know about the work of one another and made a tedious re-analysis of data taken long before, however both searches were triggered off by the authors of Ref. [4] where the resonance at  $\sim 1530$  MeV and width less than 15 MeV had been predicted.
  - [4] D. Diakonov, V. Petrov and M. Polyakov, Z. Phys. **A359**, 305 (1997), arXiv: hep-ph/9703373; arXiv: hep-ph/0404212.
  - [5] B. McKinnon *et al.* [CLAS Collaboration], Phys. Rev. Lett. **96**, 212001 (2006), arXiv: hep-ex/0603028.
  - [6] S. Niccolai *et al.* [CLAS Collaboration], Phys. Rev. Lett. **97**, 032001 (2006), arXiv: hep-ex/0604047.
  - [7] R. De Vita *et al.* [CLAS Collaboration], Phys. Rev. **D74**, 032001 (2006), arXiv: hep-ex/0606062.
  - [8] A. Titov, B. Kampfer, S. Date and Y. Ohashi, Phys. Rev. **C72**, 035206 (2005), Erratum: *ibid.* **C72**, 049901 (2005), arXiv: nucl-th/0506072; nucl-th/0607054.
  - [9] V. Guzey, Phys. Rev. C **69**, 065203 (2004), arXiv: hep-ph/0402060; arXiv: hep-ph/0608129.
  - [10] H. Kwee, M. Guidal, M. Polyakov and M. Vanderhaeghen, Phys. Rev. **D72**, 054012 (2005), arXiv: hep-ph/0507180.
  - [11] D. Diakonov, talks at *Quarks 2006* (St. Petersburg, May 19-26, 2006) and at *Quark Confinement and Hadron Spectrum VII* (Ponta Delgada, Sep. 2-7, 2006), to be published in the corresponding Proceedings, arXiv: hep-ph/0610166.
  - [12] T. Nakano, talk at the Bochum workshop on  $\eta$  photoproduction (Feb. 23-25, 2006); talk at the Internat. Conf. on Strangeness in Quark Matter (UCLA, March 26-31, 2006) and other presentations.
  - [13] V.V. Barmin *et al.* [DIANA Collaboration], arXiv: hep-ex/0603017.
  - [14] A. Kubarovsky, V. Popov and V. Volkov [for the SVD Collaboration], arXiv: hep-ex/0610050.
  - [15] R.N. Cahn and G.H. Trilling, Phys. Rev. D **69**, 011501 (2004), arXiv: hep-ph/0311245.
  - [16] R. Mizuk [for BELLE Collaboration], talk at the EPS International Europhysics Conference on High Energy Physics (Lisbon, 21-27 Jul 2005), PoS HEP2005, 089 (2006).
  - [17] R. A. Arndt, I. I. Strakovsky and R. L. Workman, Phys. Rev. C **68**, 042201 (2003) [Erratum-*ibid.* **69**, 019901 (2004)], arXiv: nucl-th/0308012;
  - A. Sibirtsev, J. Haidenbauer, S. Krewald and U. G. Meissner, Phys. Lett. B **599**, 230 (2004), arXiv: hep-ph/0405099.
  - [18] D. Diakonov and V. Petrov, Phys. Rev. **D72**, 074009 (2005), arXiv: hep-ph/0505201.
  - [19] C. Lorcé, Phys. Rev. **D74**, 054019 (2006), arXiv: hep-ph/0603231.
  - [20] A.G. Oganesian, arXiv: hep-ph/0608031.
  - [21] M. Polyakov and A. Rathke, Eur. Phys. J. **A18**, 691 (2003), arXiv: hep-ph/0303138;
  - H.-C. Kim *et al.*, Phys. Rev. **D71**, 094023 (2005), arXiv: hep-ph/0503237;
  - Ya. Azimov, V. Kuznetsov, M. V. Polyakov and I. Strakovsky, Eur. Phys. J. A **25** (2005) 325, arXiv: hep-ph/0506236.
  - [22] This upper limit was obtained assuming certain extrapolation of the data to the kinematical range experimentally unaccessible [7]. The actual upper limit for the  $\Theta^+$  production may be therefore somewhat larger.
  - [23] Ya. Azimov, V. Kuznetsov, M. Polyakov and I. Strakovsky, arXiv: hep-ph/0611238.
  - [24] T. Mibe *et al.* [LEPS Collaboration], Phys. Rev. Lett. **95** (2005) 182001 [arXiv:nucl-ex/0506015].